Finisterra, XXX, 59-60, 1996, pp. 123-138

REGIONAL THERMAL PATTERNS IN PORTUGAL USING SATELLITE IMAGES (NOAA AVHRR)(1)

M.J. ALCOFORADO(2)
S. DAVEAU(3)
A. LOPES(4)
M. BAUMGARTNER(5)

Abstract – In this paper two NOAA AVHRR diurnal images (channel 4) are used to determine the required procedures aiming at a future operational analysis system in Portugal. Preprocessing and classification operations are described. Strong correlation between air and surface temperature is verified and rather detailed air temperature patterns can be inferred.

Key-words: remote sensing, NOAA AVHRR, temperature, Portugal.

Resumo – PADRÕES TÉRMICOS REGIONAIS EM PORTUGAL, DETERMINADOS A PARTIR DE IMAGENS NOAA AVHRR. Descrevem-se as diversas fases de pré-processamento e de classificação de imagens NOAA AVHRR (canal 4: infra-vermelho térmico), a partir de um exemplo de duas cenas diurnas. Uma vez confirmada a forte correlação entre temperatura do terreno e do ar, torna-se possível inferir esta última para áreas com fraca densidade de estações meteorológicas. A variação espacial da temperatura pode ser interpretada à luz da dinâmica atmosférica nas horas precedentes à da imagem.

Palavras-chave: detecção remota, NOAA AVHRR, temperatura, Portugal.

(1) Foi apresentada uma comunicação sobre este tema no Colóquio "Climatology and Air Pollution" (U.G.I.), que teve lugar em Mendoza (Argentina), em Agosto de 1995. Reproduz-se o texto em inglês então divulgado num círculo restrito.

(2) Professora Associada da Universidade de Lisboa, Investigadora do Centro de Estudos Geográficos

(3) Investigadora do Centro de Estudos Geográficos

(4) Assistente da Universidade de Lisboa, Investigador do Centro de Estudos Geográficos. Faculdade de Letras, Cidade Universitária, 1699 Lisboa Codex. Tel: (351-1) 7940218; Fax: (351-1) 793 86 90; antlop@mail.telepac.pt.

(5) Professor Associado do Instituto de Geografia da Universidade de Berna. Hallerstr. 12, 3012 Berna, Suíça. Tel: (41-31) 631 80 20; Fax (41-31) 631 85 11

INTRODUCTION

The present study develops a method that enables the accurate drawing of thermal maps in greater detail and avoids spatial interpolation as much as possible. Thermal limits were often noticed to occur at the same locations, for a wide range of temperatures. If a relationship between air and surface temperature recorded by a satellite is verified, then remotely sensed infra-red images may be used as a tool for thermal mapping purposes (DAVEAU, 1982; CASELLES, 1991). A first experiment using diurnal NOAA images is presented.

Advanced Very High Resolution Radiometer (AVHRR) is a five-channel sensor of the NOAA series of satellite data in a sun-synchronous orbit. It records the radiation reflected and emitted by the Earth's surface and the atmosphere at spectral bands between 0.58 and 12.5µm, with a radiometric resolution of 0.12K. Pixel dimensions are 1.1 x 1.1 km at *nadir*. The approximate local over-pass time is 3 a.m. and 2 p.m.

We are aware that a great number of images are needed to achieve final representation of characteristic patterns, as in the case of the fog maps in Switzerland drawn by WANNER and KUNZ (1983), based on 94 weather satellite images. However, these two images are used to determine the required procedures, aiming at a future operational analysis system in Portugal.

I – IMAGE PROCESSING

The images were received at the University of Bern, Department of Geography (BAUMGARTNER and FUHRER, 1991). Two images were selected for evaluation, featuring diurnal scenes of the western part of the Iberian Peninsula (March 15th and August 4th 1992).

They both refer to clear conditions or to occasions of slight nebulosity. The images were processed using IDRISI 4.0 program for DOS. For geometrical correction all channels were used, but we concentrated on the thermal channels, mostly on channel 4 (10.3-11.3µm). Detailed information about land surface temperature distribution in Portugal and western Spain was derived from this analysis.

1 – PREPROCESSING

1.1 – Geometrical correction and integration of geographical attributes

Geometrical correction was carried out by comparing the images with a Lambert conical projection hypsometric map (1: 2 000 000). Structures in thermal data together with geographical features in channels 1 and 2 were used for geometrical correction. The image coordinates of prominent features (mainly the coastline, the rivers, the Tagus and the *Sado* estuaries and some dams) were stored together with the coordinates of these points in a rectified image derived from the above mentioned map. Image resampling (nearest neighbour) and geometric correction (cubic mapping function) on *Idrisi* Program were used for this purpose.

Topological data as the coastline, main rivers, boundary line between Portugal and Spain, main cities was integrated in the data set. These layers were digitised from the 1: 2 000 000 hypsometric map. The geographical layers were transferred to the image processing module and used as an overlay on each satellite image.

1.2 – Radiometric correction

The data used in this study was not corrected for atmospheric attenuation. However, cloud-free situations were selected to reduce atmospheric-induced effects. Even though the remotely sensed radiation lies in an atmospheric window region, spatially averaged measurements of surface radiant temperature without correction may not be good enough to be used as absolute values.

Channel 4 (10.3 – 11.3μ) was used more intensely because the absorption rate from water vapour is smaller than for channel 5 (11.5 – 12.5μ). The influence of CO_2 is larger on band 4 than on band 5, but it can be ignored.

Nevertheless, there is a good correspondence between brightness temperature (determined from channel 4 analysis) and air temperature in Portugal and Spain. On August 4th, the correlation coefficient between air temperature (from 25 meteorological stations in Portugal and Spain) and brightness temperature was 0.69 ($P < 0.01$).[(6)]

1.3 – Calibration

The data was calibrated using software developed at the Department of Geography (University of Bern). Surface temperatures were calculated by applying Stefan-Boltzmann's equation. Surface emissivity was considered constant.

1.4 – Image enhancement

Image enhancement techniques were used to improve the quality of the images, which was necessary for visual investigations. One of these techniques involves the stretching operation. Linear stretching with 5% saturation was carried out: a proportion (5% in this case) of very small

(6) The regression was not carried out on March 15th on account of insufficient meteorological information.

numbers of low values was forced to a minimum value; and the same proportion of a very limited number of high values was forced to the maximum value. Saturating the extremes eliminates minor features and allows the colour scale to be used more effectively to depict the majority of pixels.

2 – CLASSIFICATION

The aim of the classification procedures was to produce a thematic map with several temperature classes, to enhance the images and to guide their visual interpretation, ignoring unnecessary details and associating pixels with similar spectral signature.

A cluster analysis was carried out using unsupervised classifications from composite images (channels 3, 4 and 5). These classifications, as well as the supervised classifications, gave unsatisfactory results. For this reason, another procedure was performed, based on image analyses of channel 4 and on field knowledge: for instance, the 29 classes on the histogram in fig. 1 were grouped in 8 classes, whereas the limits between the classes were determined subjectively (fig. 1).

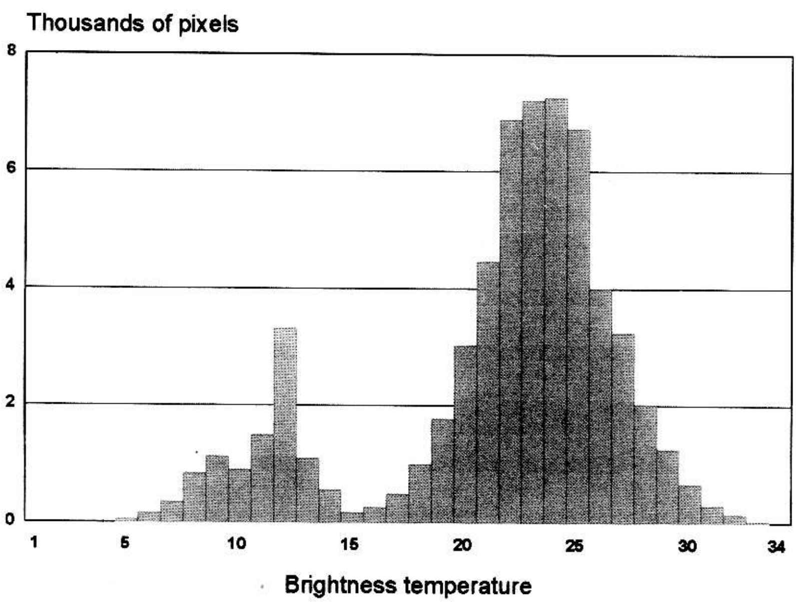

Figure 1 – Brightness temperature histogram from a NOAA 11 image, from the western part of the Iberian Peninsula (channel 4, March 15th, 1992, 14:32).

Figura 1 – Histograma das temperaturas de superfície, obtidas a partir do canal 4 da imagem NOAA 11 de 15/3/92, às 14h32.

The subjectively classified images were used for initial visual interpretation, followed by detailed analyses of stretched channel 4 images, for each date. Due to financial and space restrictions, we show colour reproductions of the non-classified stretched images only. The black and white classified image of March 15th is not reproduced either.

II – IMAGE ANALYSIS

On both August 4th and on March 15th, high pressure centres were located over the Atlantic: in August, over the Azores islands and in March, northeast of these islands. In both cases, the anticyclone also spread over western Europe. As a result of this situation, air masses moved from the East to the Iberian Peninsula. In August, however, a thermically induced pressure decrease over the Iberian Peninsula caused an inflexion of the isobars and the wind reached Portugal from the North, NW or even from the West at 6 p.m. In March, the wind blew mostly from the East before satellite over-pass time. On both occasions, wind over the Iberian Peninsula was weak (in Lisbon, at noon: 3m/s in August, 2m/s in March). Over Lisbon, there were thin low thermal inversions. Surface pressure was over 1000 hPa. On these occasions there is generally a strong West-East spatial variation of air temperature over Portugal (ALCOFORADO, 1992).

1 – INTERPRETATION OF THE IMAGE OF AUGUST 4TH 1992

The classified image (fig. 3) shows clearly a West-East temperature increase over the western part of the Iberian Peninsula. Two main exceptions are:

a)The low temperatures over southern Portugal and Spain that correspond to the tops of high convection clouds: at *Beja*, there was no nebulosity at noon, but its value increased to 6/8 at 6 p.m. There was no rain, but thunder was heard. Maximum temperature had reached 42°C at *Beja*, shortly before the image was recorded (fig. 3).

b)The temperature increase to the East is interrupted in the highlands, particularly in the mountains of the *Cordilheira Central.*

The limits between warm and cooler areas are particularly sharp on the lee-ward side of concordant mountains: northwards from Lisbon, the valleys of the Tagus right bank affluents (flowing from the West to the East) are warm, as well as the eastern slopes of the Portuguese *Estremadura* hills, sheltered from maritime air.

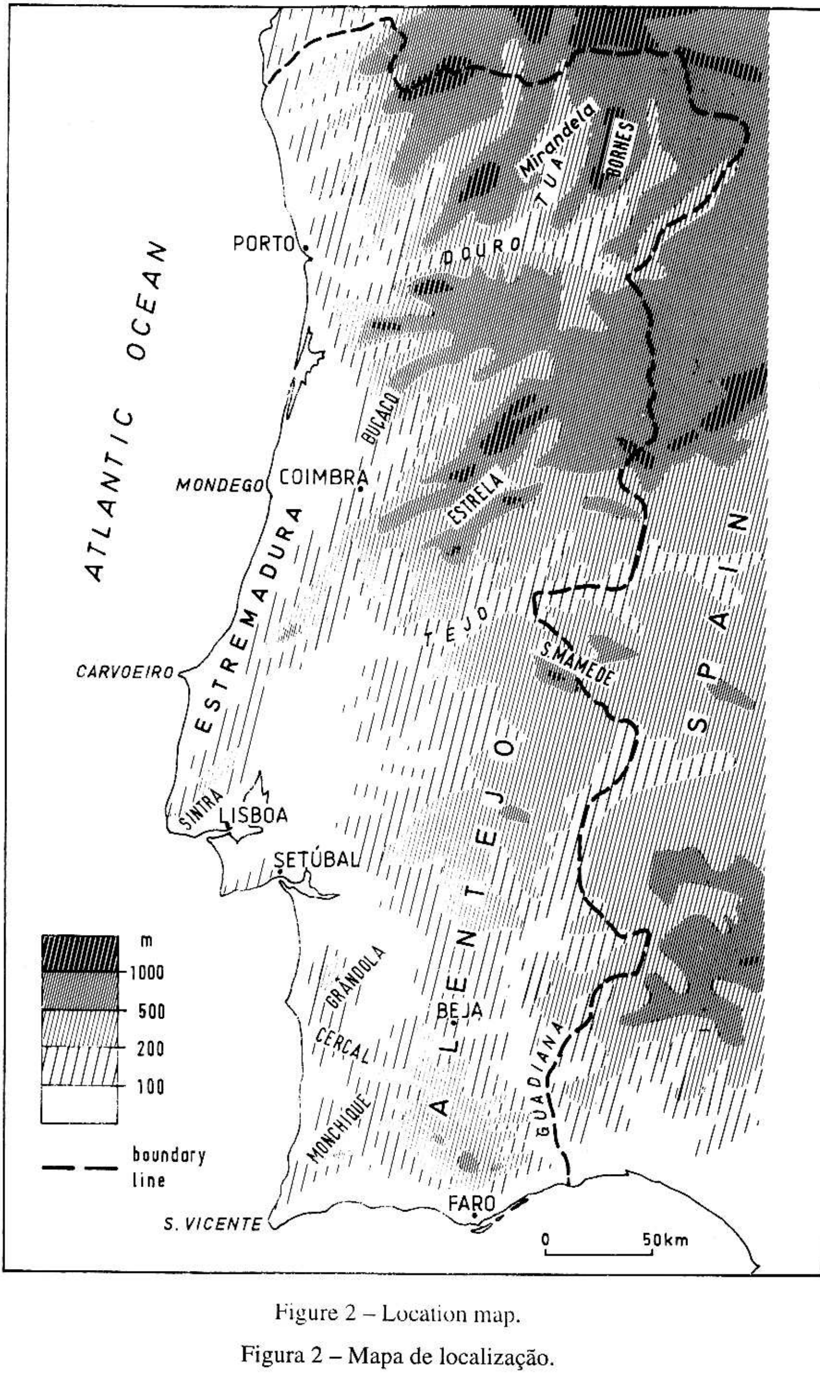

Figure 2 – Location map.

Figura 2 – Mapa de localização.

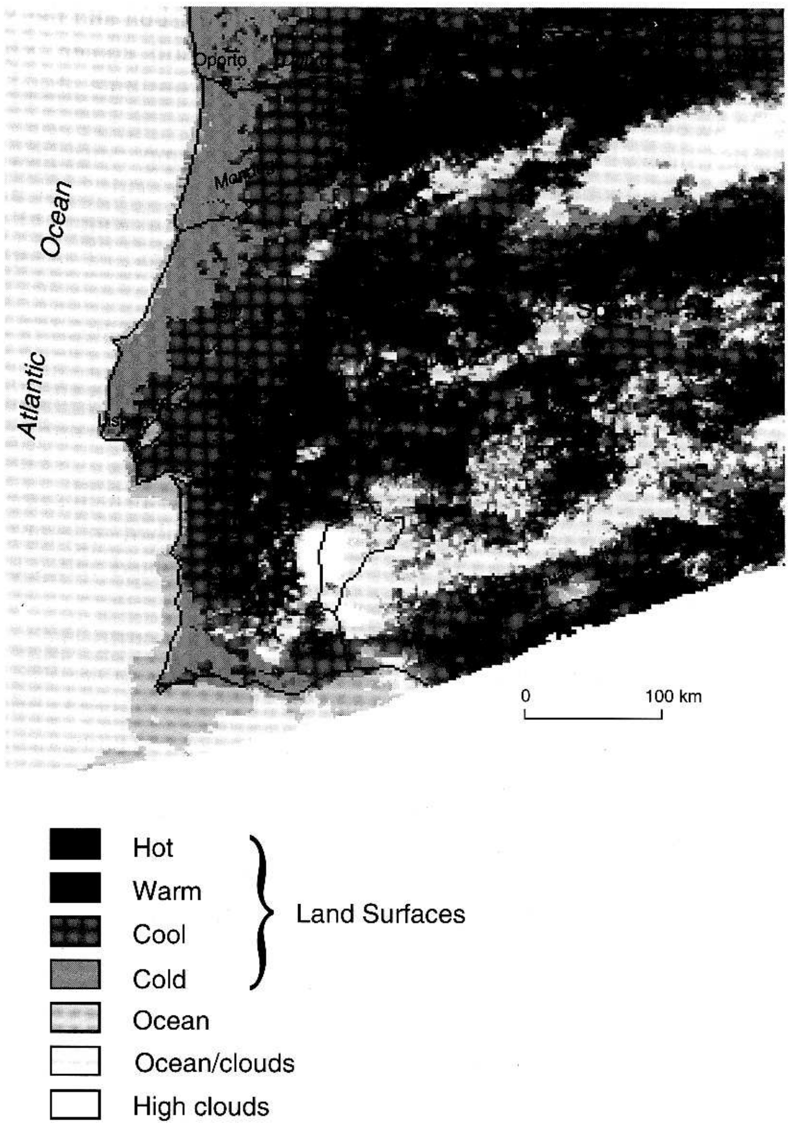

Figure 3 – Classified image from the western part of the Iberian Peninsula (channel 4, August 4th, 1992, 14:32).

Figura 3 – Canal 4 da imagem NOAA 11 de 4/8/92, às 14h32: classificação "subjectiva".

On the southwestern edge of Portugal, the influence of maritime cool air penetration is detectable through the lower surface temperatures. There is a roughly triangular cool area in SW Portugal: maritime fresh air progresses over the continent where the "shelter" effect from the Lisbon and the *Setúbal* peninsulas disappears. *Monchique* (902 m high) is still cooler. *Serra de Grândola* and *Serra do Cercal*, parallel to the littoral, constitute obstacles for maritime air inland access.

Figure 4 shows even more details. Low sea surface temperatures are found alongside the Portuguese coast northwards from Lisbon. This cold water is due to the *upwelling* system caused by frequent North winds. On these images, surface cold waters do not appear southwards from Lisbon, probably on account of a sheltered situation.

The valleys of the East-West brooks that flow into the Atlantic give way to maritime air, and they appear quite cool.

In the Northeastern part of Portugal, to the East of the *Tua* valley, a large temperature increase can be noticed, even greater on basins (*Mirandela)*. The main elevations remain cool *(Serra de Bornes,* 1199m).

The Tagus valley floor and of one of its left bank affluents (*Sorraia*) appear cool. The low surface temperature may be ascribed to evaporation, due to irrigation (rice is grown in some areas). Non irrigated valley bottoms are rather warm.

The low central area of the *Setúbal* Peninsula is very warm. The temperature may still be under-estimated on account of the low emissivity of the active surface, constituted mainly by sands (emissivity = 0.81). Empirical knowledge of this area confirms its relatively high diurnal temperatures (as well as low temperatures during winter nights).

The *Alentejo* is very warm, partly due to its isolation from the Atlantic (see concordant hills on figure 3). No details about surface temperatures are given, on account of nebulosity over this part of the country, but they must have been high, contributing to convection clouds: maximum air temperatures reached 39 °C at *Évora*, 42 at *Beja* and 43 at *Sevilla* (fig. 5). However, some higher areas (e.g. *Serra de S.Mamede*) appear cooler.

2 – COMPARISON WITH THE IMAGE OF MARCH 15TH 1992

On March 15th, the West-East temperature gradient is smaller than in August (fig. 6). Even the terminal part of the *Douro* River is rather warm, as well as the lower regions near *Coimbra*, westwards from the *Serra do Buçaco* (549m) and quite near the ocean. This considerably weak gradient often occurs when easterly light winds are recorded in most meteorological stations, confirming that the continental air is reaching the coastal areas.

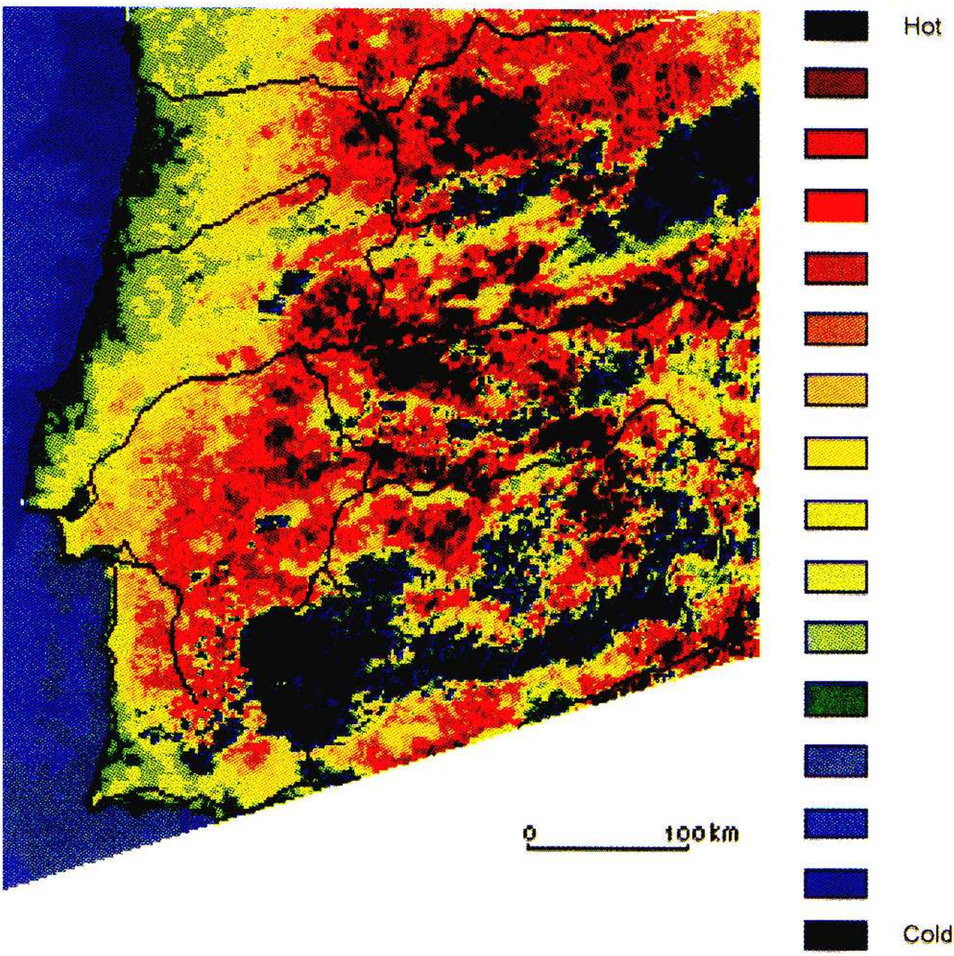

Figure 4 – Streched image from the western part of the Iberian Peninsula (channel 4, August 4th, 1992, 14:32, 5 % saturation).

Figura 4 – Canal 4 da imagem NOAA 11 de 4/8/92, às 14h32: imagem com 5 % de saturação nos valores extremos.

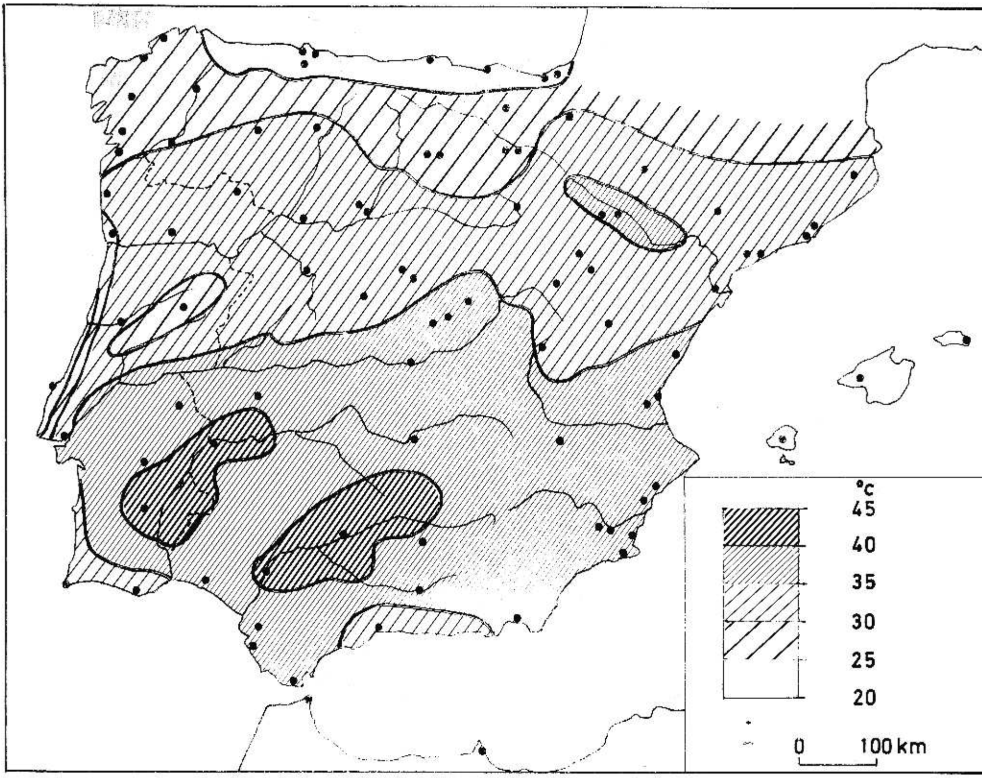

Figure 5 – Maximum air temperature on the Iberian Peninsula on August 4th 1992.

Figura 5 – Temperatura do ar na Península Ibérica a 4/8/92.

Concerning the inner areas of northern Portugal, surface temperature variation is similar to August 4th. But in March, thermal limits appear quite sharp in central and southern Portugal. As the fields of the *Sorraia* valley plain are not irrigated in March, they appear relatively warm on this image.

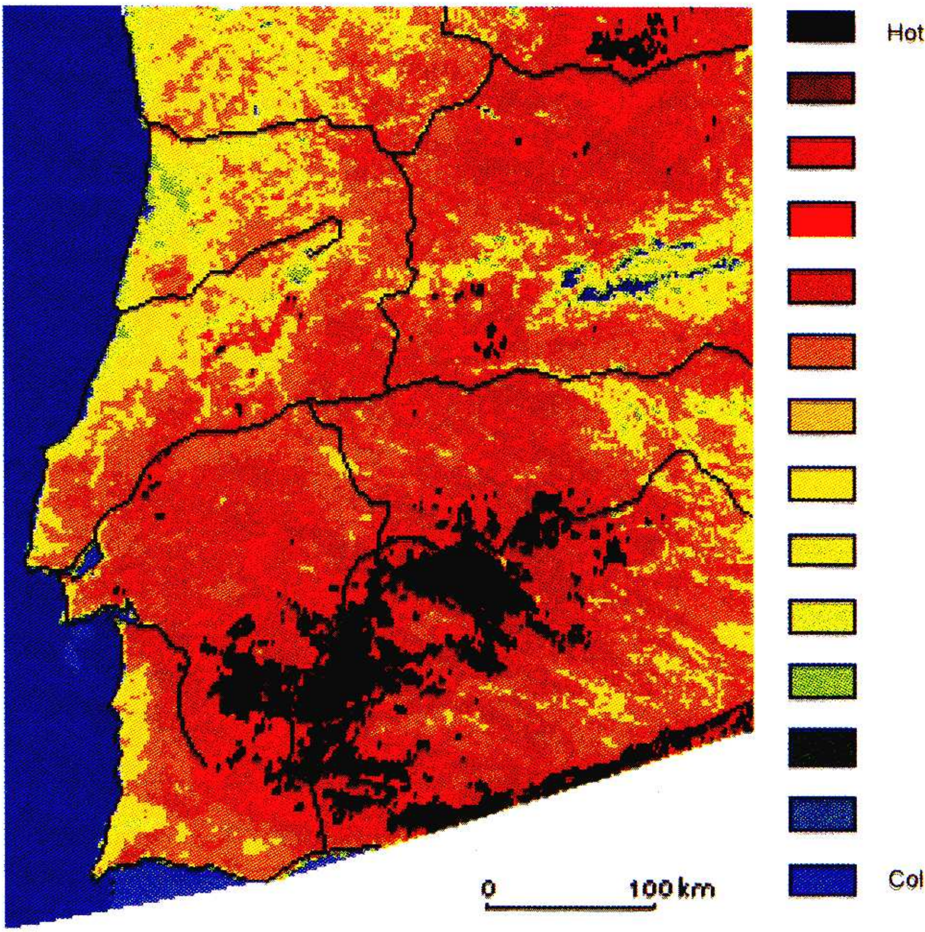

Figure 6 – Classified image from the western part of the Iberian Peninsula (channel 4, NOAA 11, March 15th 1992, 14:22).

Figura 6 – Canal 4 da imagem NOAA 11 de 15/3/92, às 14h22: classificação "subjectiva".

Southwards from *Setúbal*, the *Sado* lowlands have higher brightness temperatures than the surrounding areas. Due to the absence of clouds over the *Alentejo*, very high temperatures were recorded by the satellite. In March, a strong vertical temperature gradient could have occurred inland, although the thermal vertical gradient in Lisbon does not show it: all the hills of the Alentejo and the Algarve, some of which do not exceed 300 or 400 meters, appear clearly cooler on this image, separated by very warm depressions.

In western Algarve, 902m high *Serra de Monchique* protects its lee area from Atlantic fresh air masses, which was not the case in August.

III – LAND SURFACE TEMPERATURE VERSUS GEOGRAPHICAL FACTORS

The calculation of a numerical relationship (regression analysis) between land surface temperature (LST) and geographical factors was carried out for a small area (fig. 7), where Lisbon's area is included, taking into consideration a latitudinal factor and a longitudinal factor. These two factors were determined from a grid, whose origin is situated southwest from Portugal. Some of the correlation coefficients are shown on table 1.

Table 1 – Correlation and determination coefficients between brightness temperature and two geographical factors (latitude, longitude)

Quadro 1 – Coeficientes de correlação e de determinação entre a temperatura do terreno e dois factores geográficos (latitude e longitude)

		Correlation coefficient (R)	Determination coefficient (R^2)
15.03.1992	Latitudinal factor	0.18	0.03
15.03.1992	Longitudinal factor	0.84	0.71
4.08.1992	Latitudinal factor	0.35	0.13
4.08.1992	Longitudinal factor	0.73	0.53

There is no significant linear relationship between LST and latitude (0.18 and 0.35, table 1). For this area, still lower correlation coefficients were obtained when LST was replaced by air temperature values (table 2); it must be stated that for air temperature regressions only 28 meteorological stations were used, whereas for LST we worked with thousands of pixels (512 x 512).

In contrast, the correlation coefficients between temperature and longitude were quite high and positive for diurnal LST (0.84 in March, 0.73 in August) as well as for air temperature (0.69), both increasing inland.(7)

(7) In winter nights, the coefficients were negative (0.75 on January 5th, temperature decrease with distance inland).

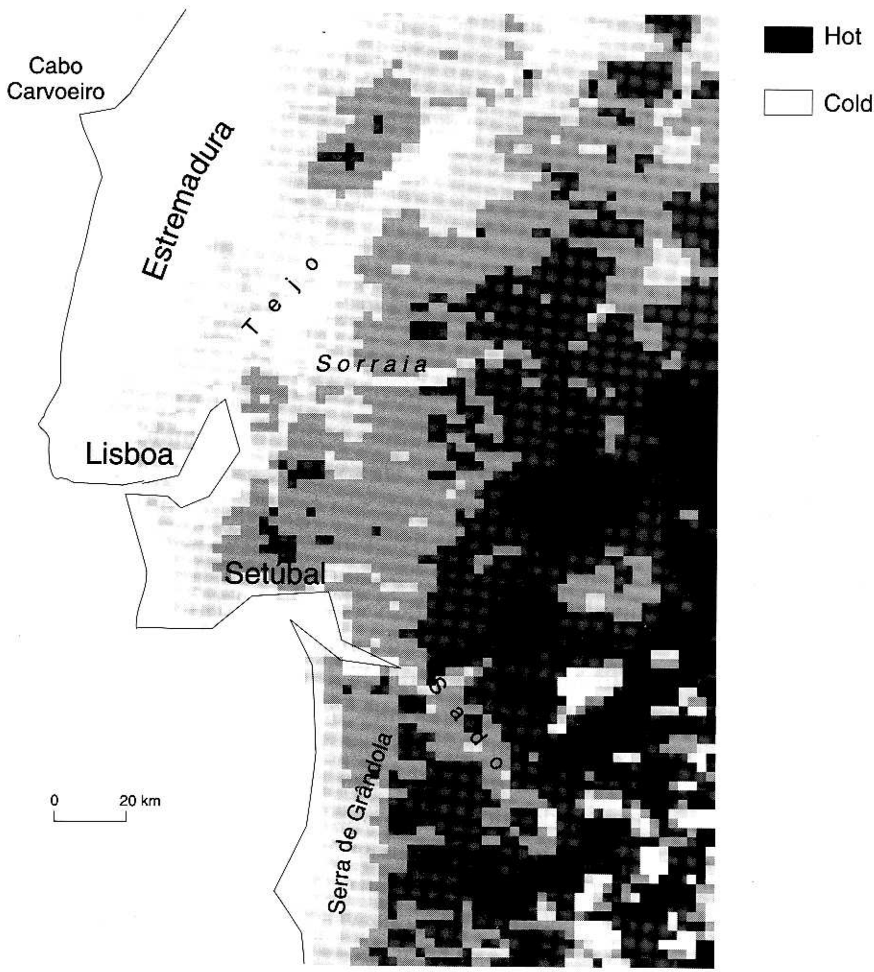

Figure 7 – Enlarged image from August 4th 1992.

Figura 7 – Ampliação da imagem de 4/8/92: a região de Lisboa.

Although Portugal is quite narrow, West-East air and land surface temperature variations (increase during the day and decrease at night) are greater than South-North temperature reduction.

The greater residual values occur in high altitude regions. Concerning air temperature, altitude is the most important factor modifying its variation, except in the summer, when the correlation with distance inland is higher than with altitude (table 2).

Table 2 – Correlation coefficients (R) between March and August mean maximum air temperature and geographical factors. Significative values ≥ 0.44 (P ≤ 0.02) (Source: Alcoforado, 1992)

Quadro 2 – Coeficientes de correlação entre as temperaturas máximas médias de Março e de Agosto e três factores geográficos

	March	August
Latitudinal factor	-0.02	-0.15
Longitudinal factor	0.69	+0.86
Altitude	-0.76	-0.44

CONCLUSION AND FURTHER RESEARCH

The procedures necessary for a future operational analysis system of NOAA AVHRR images were described. The preprocessing operations will be sistematically repeated (geometrical correction by comparison of the images with a Lambert conical projection hypsometric map, calibration, image enhancement by linear stretching with 5% saturation). Image classification for the purpose of guiding visual interpretation will remain partially subjective.

A strong **correlation between air and surface temperature was verified.** This fact enabled us to **infer detailed thermal information** concerning areas with no meteorological stations, especially in mountainous regions, where previously interpolation has been the sole tool used in climatological temperature map drawing (DAVEAU *et al*, 1985). For any area, it is now possible to produce a relatively more detailed map. The knowledge of detailed thermal patterns is also very useful for regional planning projects and impact studies. Their usefulness is nevertheless limited by pixel dimension.

The interpretation of spatial temperature variation on several occasions led to the **understanding of regional and local air dynamics** during a period of time before the image was recorded. Some examples are mentioned above (hills that constitute obstacles to the penetration of maritime air masses, valleys driving cool and humid Atlantic air inland, etc.).

Another conclusion draws on the evidence that the **correlation coefficients between land surface temperature** and **latitude** on the one hand, and land surface temperature and **longitude** on the other, were similar to those obtained when using air temperature values. Therefore, the correlation between air and surface temperature is indirectly proved. LST dependence on ground cover is not sufficiently high to rub out the effect of air temperature variation, except in the case of irrigated areas.

Our next goals will be to derive a map indicating the more frequent influence of relief features on spatial temperature variations, and to create gradient maps, which may guide the interpolation of thermal data from meteorological stations. This, however, cannot be acheived without the study of many other satellite images: even in anticyclonic situations, thermal gradients are not always similar. On some occasions, like the ones shown in figures 3, 4 and 7, West-East temperature gradient is rather vigorous. In contrast, thermal variation is weaker on figure 6. This is even more apparent during heat waves with southeasterly or easterly winds, when hot and dry air masses may reach the coast (DAVEAU, 1982). Only a systematic image analysis will allow us to reach a synthetic scheme.

ACKNOWLEDGMENTS

The University of Bern, Department of Geography must be thanked for the offering of four NOAA images, two of which are presented here, and for receiving one of the Portuguese authors. Our thanks go particularly to Professor Heinz Wanner, Professor Michael Baumgartner and Torbjorn Holzer. We hope to be able to carry out the second part of this work using images received in Portugal.

The present work was part of a project called *Imagens e Representações para o Ordenamento Biofísico em Ambiente Urbano: Lisboa*, PBIC/C/CEN/1051/92, which was financed by the Junta Nacional de Investigação Científica e Tecnológica. We are greatful to Professor Maria Eugénia MOREIRA for reviewing the manuscript.

REFERENCES

ALCOFORADO, M.J. (1991) – Influence de l'advection sur les champs thermiques urbains à Lisbonne. *Publications de l'Association Internationale de Climatologie*, 4: 29-35.

ALCOFORADO, M.J. (1992) – *O Clima da região de Lisboa. Contrastes e Ritmos térmicos*. Memórias do Centro de Estudos Geográficos, nº15, Lisboa.

BAUMGARTNER, M.; M. FUHRER (1991) – A Swiss AVHRR and Meteosat receiving station. *Proceedings of the 5th European AVHRR User's Meeting*, EUMETAST P-09: 23-33.

CASELLES, V. (1991) – Analysis of the heat-island effect of the city of Valencia, Spain, through air temperature transects and NOAA satellite Data. *Theor. Appl. Climatology*, 43: 195-203.

DAVEAU, S. (1982) – Les températures des 3 et 4 Juillet 1978 au Portugal et dans l'Ouest de l'Espagne d'après les satellites Météosat et HCMM. *Finisterra. Revista Portuguesa de Geografia*, XVII (33): 53-96.

DAVEAU, S. et al. (1985) – *Mapas climáticos de Portugal. Nevoeiro e Nebulosidade. Contrastes térmicos*. Memórias do Centro de Estudos Geográficos, nº7, Lisboa.

SCHMID, B. et al. (1991) – Temporal evolution of vegetation index and atmospheric effects. *Preprints of EARscl Symposium*, Graz, 3-5 July.

WANNER, H. *et al.* (1983) – Klimatologie der Nebel- und Kaltluftkorper im Schweizerischen Alpenvorland mit Hilfe von Wettersatellitenbildern. *Arch. Met. Geoph. Biocl.*, Ser.B, 33: 31-56.